

The ALICE silicon drift detectors: Production and assembly

S. Beolè^{a,*}, B. Alessandro^b, S. Antinori^c, S. Coli^b, F. Costa^e, E. Crescio^b, D. Falchieri^c,
R. Arteché Diaz^{d,1}, S. Di Liberto^d, G. Giraud^b, P. Giubellino^b, G. Masetti^b, G. Mazza^b,
F. Meddi^d, F. Prino^b, A. Rashevsky^c, L. Riccati^b, A. Rivetti^b, S. Senyukov^a, L. Simonetti^b,
L. Toscano^b, F. Tosello^b, G.M. Urciuoli^d, A. Vacchi^c, R. Wheadon^b

^aUniversità di Torino/INFN, Torino, Italy

^bINFN, Torino, Italy

^cINFN, Trieste, Italy

^dUniversità di Roma "La Sapienza"/INFN, Roma, Italy

^eUniversità di Bologna/INFN, Bologna, Italy

Available online 1 August 2007

Abstract

Silicon Drift Detectors (SDDs) have been selected to equip the two intermediate layers of the Inner Tracking System (ITS), of the ALICE experiment, since they couple a very good multitrack capability with dE/dx information and excellent spatial resolution as described in references. In this paper we describe the different components of the SDD system as well as the procedures of the system assembly.

© 2007 Elsevier B.V. All rights reserved.

PACS: 25.75.-q; 29.40.Gx; 29.40.Wk

Keywords: Silicon drift detectors; Microcables; TAB bonding

1. Introduction

The ALICE ITS, as described in detail in Refs. [1,2], consists of six layers of silicon detectors. Because of the high particle density, up to 90 cm^{-2} , the four innermost layers ($r \leq 24\text{ cm}$) must be truly two-dimensional devices. For this task silicon pixel and silicon drift detectors (SDDs) were chosen. The outer two layers at $r \approx 45\text{ cm}$, where the track densities are below 1 cm^{-2} , will be equipped with double-sided silicon microstrip detectors. The ALICE SDDs, $7.0 \times 7.53\text{ cm}^2$ active area each, are mounted on linear structures called ladders, each holding six detectors for layer 3, and eight detectors for layer 4. The layers are composed of 14 and 22 ladders and sit at the average radius of 14.9 and 23.8 cm, respectively. The front-end electronics

is mounted on rigid heat-exchanging hybrids, clipped onto cooling pipes running along the ladder structure. The large number of channels in the layers of the ITS requires a large number of connections from the front-end electronics to the detector and to the readout. The requirement for a minimum of material within the acceptance does not allow the use of conventional copper cables near the active surfaces of the detection system. Therefore TAB bonded aluminum multilayer microcables are used. This type of cables are produced by the Scientific Research Technological Institute of Instrument Making Microelectronic Department, Ukraine, and are used both for signal and power supply lines. A detailed description can be found in Ref. [3]. The same technology is used to connect the detector and its read-out hybrids to the interface boards placed at the two ends of the ladder.

2. The SDD module

An SDD module (see Fig. 1) consists of one silicon drift detector, two front-end hybrids each connected to the

*Corresponding author.

E-mail address: beole@to.infn.it (S. Beolè).

URL: <http://www.ph.unito.it/~beole/> (S. Beolè).

¹On leave of absence from CEADEN, Havana, Cuba.

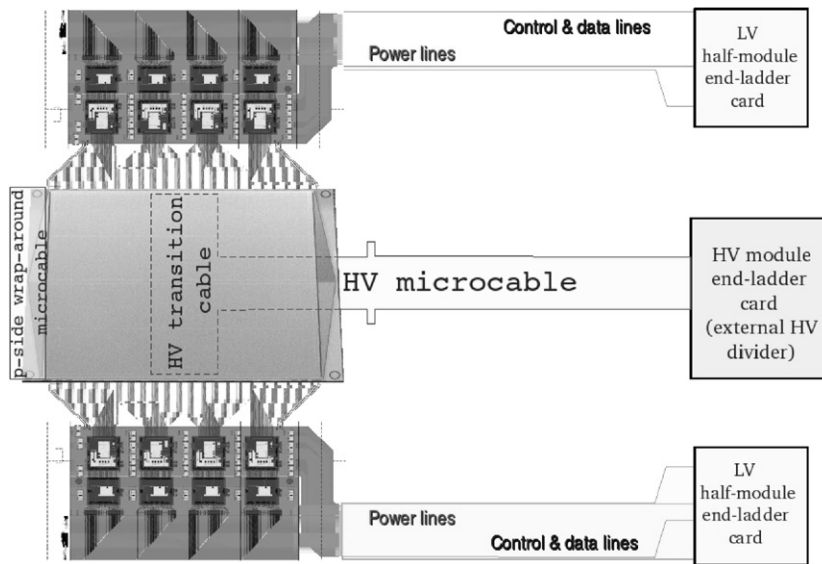


Fig. 1. SDD module scheme.

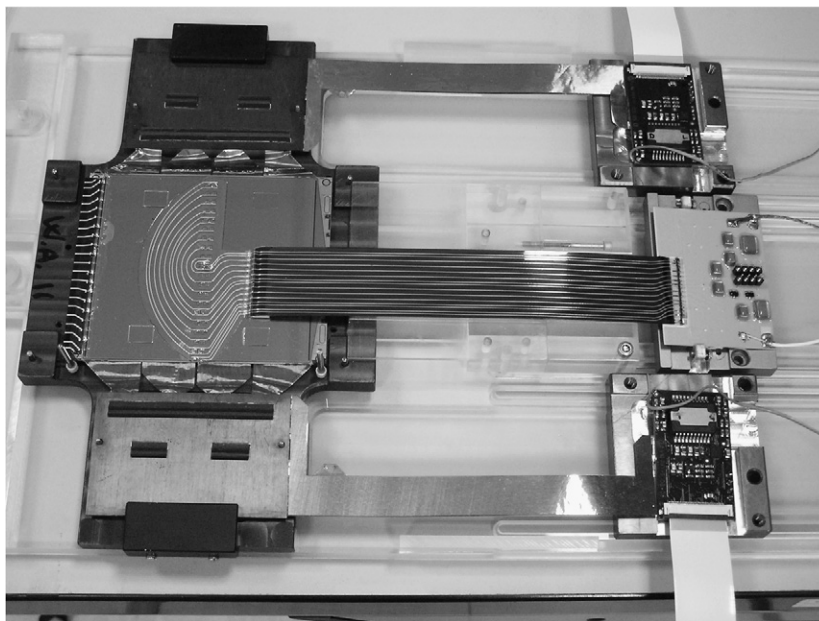


Fig. 2. Picture of a complete SDD module.

corresponding end-ladder LV boards and a microcable specially designed to carry high voltage (up to 2.4 kV) which connects the detector to the HV end-ladder board. All the assembly steps are performed in the Technology Laboratory of INFN Torino. The final assembly is visible in Fig. 2.

2.1. Sensor

The detectors are produced on 5-in. diameter neutron transmutation doped (NTD) silicon wafers with resistivity of 3 kΩcm and a thickness of 300 μm. The detector has a

bidirectional structure, where electrons drift from the central p⁺ cathode toward two linear arrays of 256 anodes (anode pitch 256 μm). The length of the sensitive area is 70.0 mm, and the sensitive-to-total area ratio is 83%. The detailed description can be found in Ref. [4]. The detector bias voltage is provided by specially designed microcables. The connections to the central bias cathode and to the injector lines is provided by microcable called *transition cable*, glued on the detector p-side. The bias lines are then bonded to the corresponding bonding pads. The high voltage is then brought to the n-side using the so-called *wrap-around cable*. The transition cable is then TAB

bonded to the long HV cable connected to the corresponding HV end-ladder board. Each sensor was carefully tested in INFN Trieste and after being accepted for modules production it was equipped with *transition* and *wrap-around cables* and sent to Torino for the module assembly.

2.2. The front-end electronics

The front-end electronics, fully developed in the VLSI Laboratory of INFN Torino, consist of two integrated circuits both designed in the 0.25 μm CMOS technology. The first one, named PASCAL, performs the preamplification of the signals, their analog storage at a sampling frequency of about 40 MHz, and the analog-to-digital conversion. The second integrated circuit, AMBRA, is a digital four-event buffer which allows data derandomization and handles the communication protocol. A detailed description of the SDD front-end system can be found in Ref. [5]. The production of 48 8-in. wafers holding about 150 potentially good pairs of PASCAL and AMBRA finished in 2004. The validation tests started in the CL100 CleanRoom of INFN Rome, using a Cascade Rel-6100 Probe station, in February 2005. The yield for AMBRA was 74%, while for PASCAL was 89%. At the end of November 2006, ~ 3000 AMBRA and ~ 3000 PASCAL were available for assembly. Each SDD is coupled to two hybrids each consisting of four couples of PASCAL and AMBRA chips. Each couple of chips is TAB bonded to a circuit printed on an aluminum multilayer microcable called *chip-cable*. This circuit provides connections of data lines between AMBRA and PASCAL as well as the connections to the sub-hybrid circuit. The bondings on the chip-cables are protected by a thin layer of glue, a thermally conductive two-component alumina-filled epoxy (adhesive H70E-2), dispensed automatically with a Champion 3700 glue dispensing machine. The production yield of chip cables at the beginning of the production phase was very high both before and after the encapsulation process ($\sim 90\%$). Unfortunately in Spring 2006 some problems arose and since then the production yield went down to $\sim 70\%$. The reason of the high number of bad chip-cables (mainly due to Pascal problems) is still not well understood, and it can be found in the TAB bonding phase as well as in the thinning and dicing of the wafers. At the end of November 2006 we had bonded more than 3000 chip-cables instead of the foreseen 2400. After the encapsulation process the chip-cables are glued on a sub-hybrid circuit. The relative alignment of the four chip-cables needed for each hybrid is obtained using the SDD anodes array as a reference. The sub-hybrid is glued onto a rigid carbon-fiber heat-dissipator called *heat-bridge*. This will be clipped to the cooling tubes running along both sides of a ladder. Due to the large number of bonds on the hybrids it is very important to avoid that the inevitable occasional weak bonds lead to failure of the hybrid after only a few operational cycles. For this purpose, and following the experience of the ALICE SSD development [3], a thermal

cycling test has been introduced in the production sequence. Sample hybrids have been demonstrated to withstand 200 thermal cycles from 20 to 65 $^{\circ}\text{C}$ (the likely extremes that the hybrids can be expected to experience), and survive 10 cycles up to 100 $^{\circ}\text{C}$ despite the mismatch in the thermal expansion coefficients between the different layers of the hybrid. The hybrids are therefore exposed to 10 thermal cycles from 20 to 65 $^{\circ}\text{C}$.

2.3. Modules production and tests

At the end of November 2006, 300 modules have been assembled and tested. The assembly procedure is composed by more than 20 steps. Each TAB bonding phase is followed by encapsulation of bonds by means of different kinds of glue. After each bonding step and before glue protection, an electrical test is performed to ensure the validity of electrical connection and exclude any damaging of the components. The complexity of the assembly and test procedures leads to an average time of 3 days to have the complete module ready for final test with laser. This laser test was developed to get a complete map for the doping fluctuation for each detector. The non-uniformity of doping concentration leads to non-uniformity of drift field i.e. to non-linear trajectory of the electron cloud as well as variations of drift speed as explained in Ref. [2]. This problem has been studied carefully in the beam tests and the results published in Ref. [6]. The test set-up uses a laser source to inject charge in a known position of the detector and extract the map of residuals both along the drift and the anode directions. Only four modules turned out to have residual values up to 400 μm , similar to those observed in the past, in the beam-test data; in Fig. 3 the

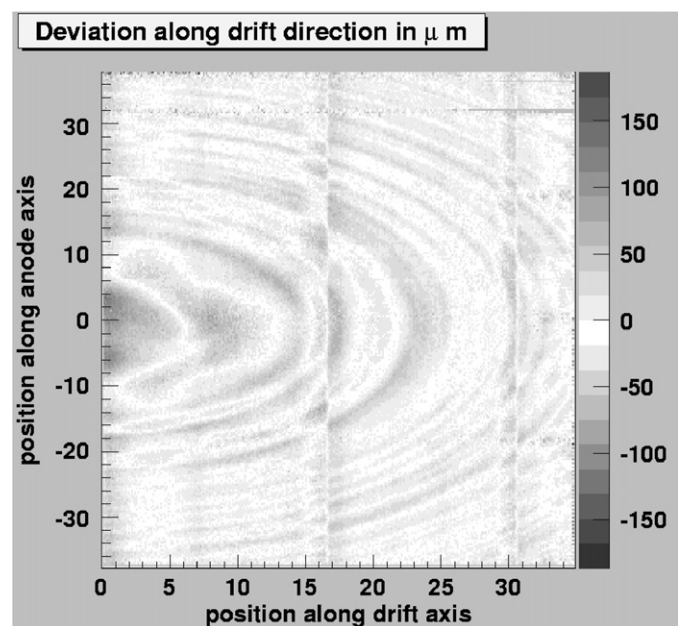


Fig. 3. Maps of residuals in a detector with doping fluctuations: please note the typical shape of dopant distribution.

typical map of residual for this kind of detector is shown. The laser test set-up constituted also a complete functioning test of the modules. It was used to detect any kind of problem both in the front-end electronics and in the sensor, as well as to detect noisy and dead channels

3. Assembly of ladders

Each SDD module is handled using a special box equipped with vacuum holders. In fact the different elements of each module (sensor, hybrids, end-ladder

boards) are connected one to the other by microcables, resulting in a completely flexible structure. Thus each element needs to be firmly held while handling to avoid mechanical stress on TAB bonding connections. The potential weakness of this connections, even if protected by glue deposition, is one of the critical points of the SDD system. A special mechanical tool has been developed to position and align SDD modules, as visible in Fig. 4.

It consists of eight supports for the sensors that can be moved in the z coordinate to allow the positioning of

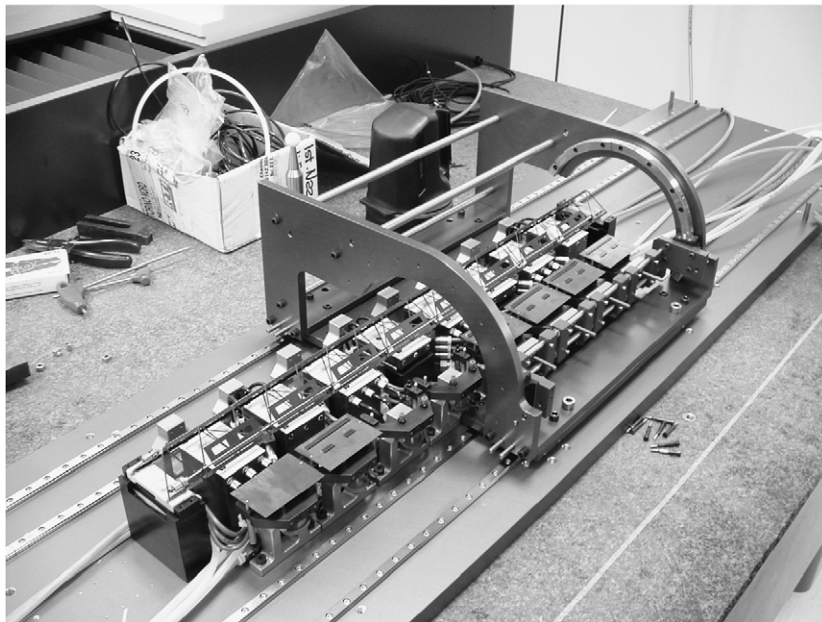


Fig. 4. The ladder assembly jig: the eight supports for sensors and the hybrid folding tool.

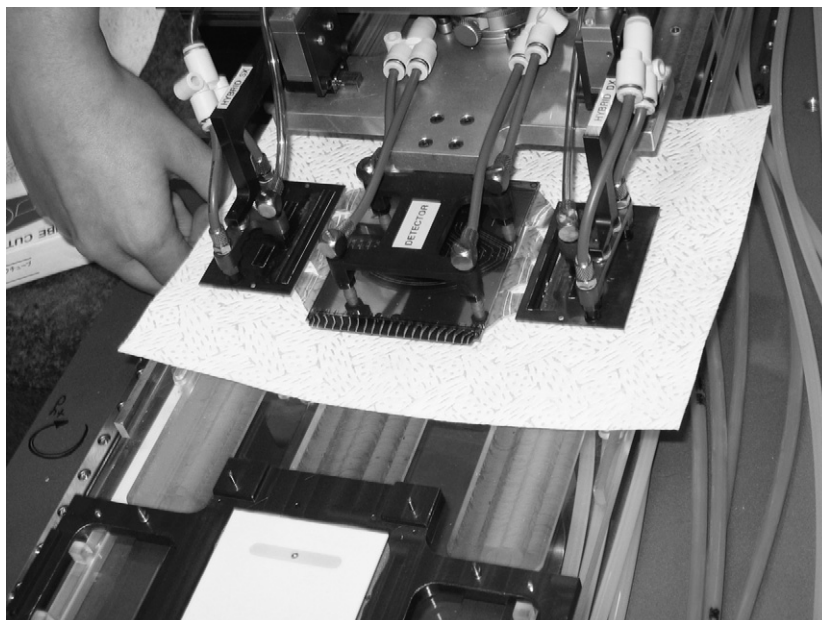


Fig. 5. The tool for module positioning.

overlapping detectors. The SDDs are positioned so that the electrons drift orthogonally to the beam axis. The anodes therefore are aligned along the ladder length. The modules

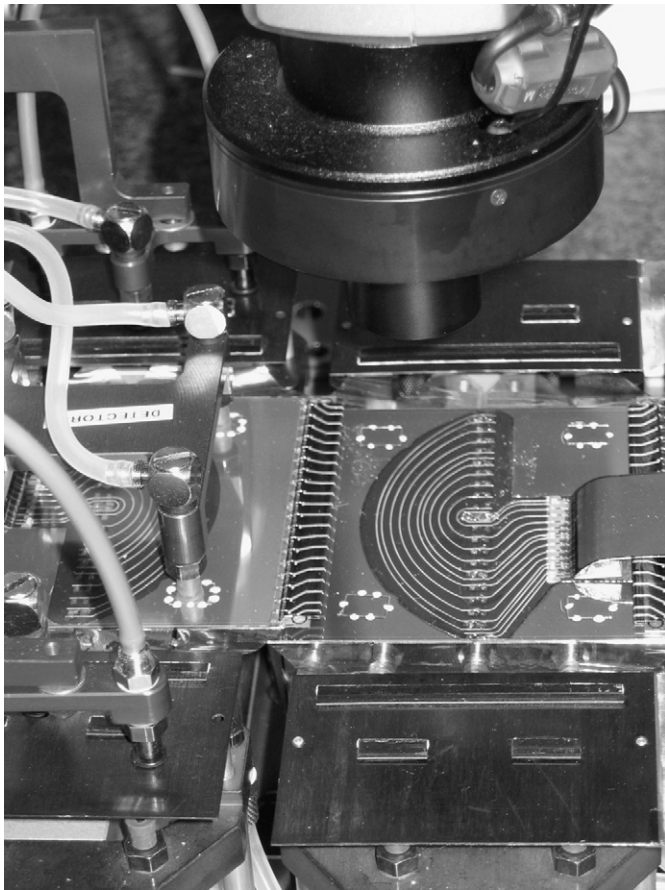


Fig. 6. The Mytutoyo video-camera while measuring reference crosses on an SDD.

are mounted at different distances from the ladder structure both in the $R\phi$ and in the Rz planes. This is in order to allow the overlap of the guard regions and a small overlap of the active areas. Each module is lifted by a tool equipped with vacuum cups which can be moved along the structure and places it on the corresponding base, visible in Fig. 5. Using the same tool the end-ladder boards are placed on dedicated supports, ready to be folded in their final configuration. After being placed on its base each SDD must be aligned. The alignment is performed using the Mytutoyo measuring machine in INFN Torino Technological Laboratory. In Fig. 6 the video-camera used in the alignment procedure is shown. It is used to measure the position of one of the reference crosses on the detector with respect to the main reference point, a ruby sphere placed on the ladder foot.

The ruby sphere is also used for ladder positioning on the ITS support structure. The positioning and alignment operation must be repeated 6 times for each ladder for ITS layer 3, and 8 times for each ladder for ITS layer 4. In Fig. 7 we show six aligned modules leaning on the corresponding bases and the ladder already placed above them.

Once the ladder is placed on the modules four small pillars are glued to each SDD. In the last phase we fold the hybrids and the LV microcables, then clip the heat-bridges to the cooling tubes and place the end-ladder boards, one HV and two LV for each module, in their final position (see Fig. 8).

The ladder production rate reached a maximum of one ladder per day, with an average value of 3–4 ladders per week. Due to different problems (one module broken during alignment, some modules with TAB bonds on the



Fig. 7. The SDD ladder placed on the six aligned modules (ITS layer 3).

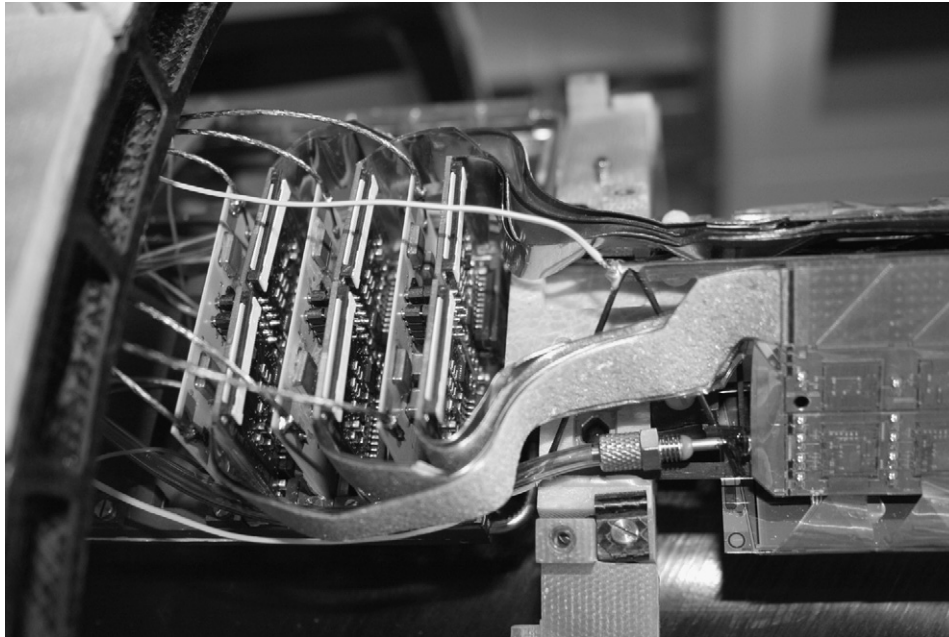


Fig. 8. End-ladder boards.

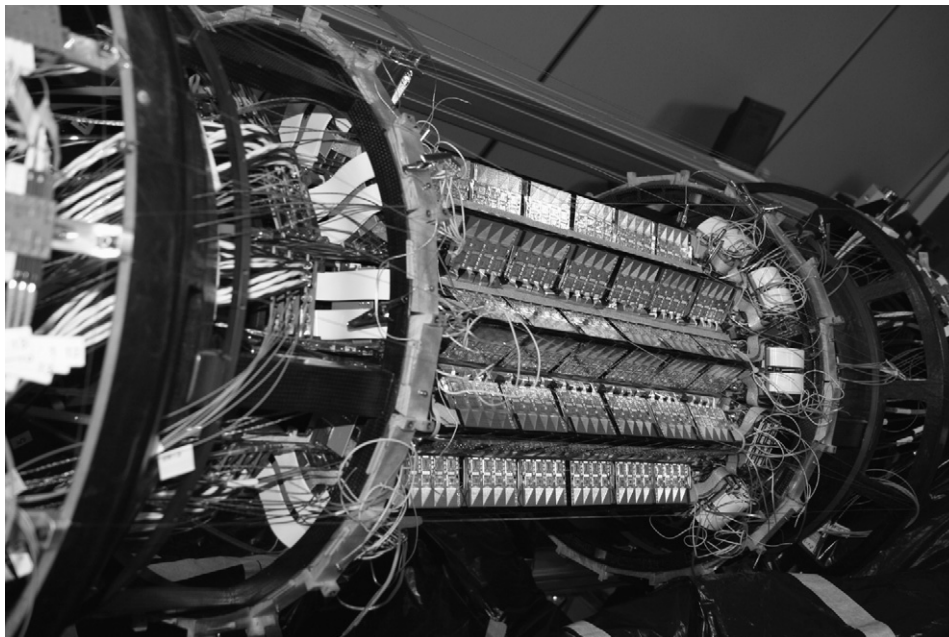


Fig. 9. Five SDD ladders of layer 3 mounted on the carbon-fiber support structure.

LV end-ladder boards broken during folding of microcables) we had to repair six ladders (four of layer 3 and two of layer 4) replacing damaged modules with good ones. At the end of November 2006 all the 14 ladders of layer 3 and 18 of layer 4 were ready to be for being mounted on the cones. In Fig. 9 you can see five ladders of layer 3 mounted on the cones (for a brief description of the carbon fiber support structures see Ref. [7]) and ready for tests.

References

- [1] ALICE Collaboration, Technical Design Report, CERN/LHCC 99-12.
- [2] S. Beolè, et al., Nucl. Instr. and Meth. A 377 (1996) 393.
- [3] A.P. de Haas, et al., in: Proceedings of the Eighth Workshop on Electronics for LHC Experiments, Colmar, September 2002.
- [4] A. Rashevsky, et al., Nucl. Instr. and Meth. A 461 (2001) 133.
- [5] A. Rivetti, et al., Nucl. Instr. and Meth. A 541 (2005) 267.
- [6] E. Crescio, et al., Nucl. Instr. and Meth. A 539 (2005) 250.
- [7] S. Beolè, et al., Nucl. Instr. and Meth. A 570 (2007) 236.